Chemical Degradation of Wooden Components in Traditional Dwelling No. 9, East Gate Lane, Gulian Village: Assessed by Polarized Light Microscopy, Fluorescence Microscopy, and Histochemical Staining

Haidi Ji ,# Tongyu Xu,# Xianghe Liu,# Ziyan Luo, Bin Li, and Yan Yang *

To accurately elucidate the microscopic degradation characteristics and deterioration mechanisms of wooden components in traditional northern Chinese dwellings, this study investigated wooden components retrieved from the Ming-Qing residential building at No. 9, East Gate Lane, Gulian Village, Qi County, Shanxi Province. Polarized light microscopy, fluorescence microscopy, and histochemical staining techniques were employed to qualitatively assess the degradation degrees of cellulose and lignin in six wood species: elm, poplar, willow, birch, Chinese larch, and Chinese pine. Internal and external deterioration drivers were analyzed, and corresponding conservation strategies were proposed. The results showed that all tested wooden components exhibit moderate to severe chemical degradation. The deterioration of wooden components is synergistically driven by interspecific differences in natural decay resistance, rainwater erosion, ultraviolet radiation, building structural damage, and microbial infestation. Elm components are mainly attacked by white-rot fungi, while the other wood species are predominantly affected by soft-rot fungi. Poplar and willow are more susceptible to insect damage. This study provides a scientific basis and technical support for the microscopic diagnosis, precise restoration, and preventive conservation of Ming-Qing wooden architecture in the Jinzhong region.

DOI: 10.15376/biores.21.4.9351-9372

Keywords: Traditional dwelling; Gulian village; Chemical degradation of wooden components; Polarized light microscopy; Fluorescence microscopy; Histochemical staining

Contact information: School of Architecture, Nanyang Institute of Technology, Nanyang, China;
*#These three authors contributed equally to this work; *Corresponding author: yangyanrainy@163.com*

INTRODUCTION

Traditional villages are tangible carriers of agrarian civilization, preserving historical heritage and architectural wisdom. Strengthening the protection and inheritance of traditional villages and buildings is a critical pathway to advance the creative transformation and innovative development of traditional Chinese culture (Li *et al.* 2024). Gulian Village, located in Qi County, Jinzhong City, Shanxi Province, is a national-level historical and cultural village and a traditional Chinese village. First established in the early Hongwu reign of the Ming Dynasty, it was originally named Kulue Village. Following the construction of a fortified village enclosure in the 20th year of the Jiajing reign (1541), it was renamed Kulue Fortress. It adopted the name Gulian Fortress in the early Qing Dynasty, and earned the prestigious moniker "Silver Gulian" after the Qianlong reign period. Currently, it preserves over 40 Ming-Qing merchant residences and public

buildings. It is predominantly of brick-wood structure with exquisite brick, wood, and stone carvings. This village is a rare physical example for systematic research on the architectural systems, craft inheritance, and cultural connotations of traditional dwellings in Jinzhong and northern China, holding significant historical and cultural value (Li 2017).

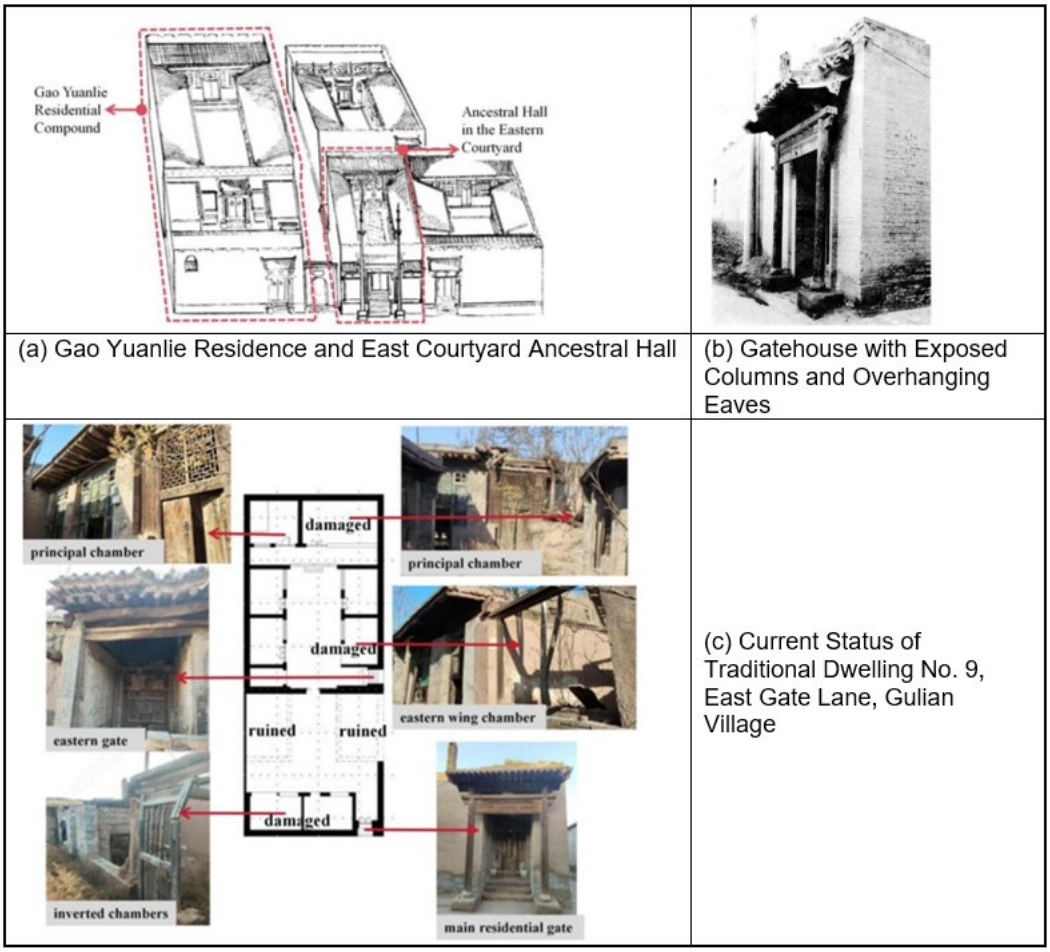

Fig. 1. Past and present of Traditional Dwelling No. 9, East Gate Lane, Gulian Village

Traditional Dwelling No. 9, East Gate Lane, originally the residence of Gao Yuanlie, sits at the southern entrance of Pawnshop Lane in East Gate Lane, Gulian Village. It consists of a residential courtyard and a family ancestral hall (Fig. 1a). Located at the core of the Ming-era Gulian Fortress, its initial construction is dated to the Hongwu–Yongle period by inference, aligned with the center-outward expansion rule of ancient Chinese village planning. As the village's sole architectural complex integrating structures from both dynasties, it holds great historical and cultural significance. The western residential section is a two-courtyard complex facing south, and its inner courtyard dates to the Ming Dynasty. The entire complex is roughly rectangular. Both the main gate and the second gate are exposed-column overhanging gatehouses. This architectural form is common and representative in traditional Chinese architecture. It uses exposed columns as structural supports and features outward-extending roof eaves, integrating structural function, practicality, and artistic decoration (Fig. 1b). This section contains 26 rooms. The eastern section served as the family ancestral hall with 15 rooms. A pair of flagpoles

originally stood in front of its gate (Fig. 1a), but they have been destroyed. Currently, only the western residential courtyard of Traditional Dwelling No. 9 remains, and its overall layout is relatively well preserved. However, severe structural damage has been observed. The east and west wing rooms of the first courtyard have been destroyed. The courtyard walls, the roof system of the inverted house, the eastern section of the main hall, and the southern part of the east wing have collapsed. Although the main gate, archway, and west wing remain relatively intact, they also show varying degrees of deterioration (Fig. 1c). These damages pose a serious threat to the structural safety and long-term preservation of the building. Currently, Traditional Dwelling No. 9 remains chronically vacant, with its collapsed and deteriorated structural elements yet to receive timely stabilization and repair. In accordance with the follow-up conservation and development plan for Gulian Village, the renovation of this courtyard complex is expected to commence in the near future.

The load-bearing structure of the residential building at No. 9 Dongmenli Courtyard is predominantly wooden, and its structural damage is primarily caused by the deterioration and degradation of wooden components. Wooden structure deterioration results from the combined action of multiple factors and is essentially a coupling process between the inherent properties of wood and external environmental stresses. The species-specific characteristics of wood form the intrinsic basis for its decay resistance and structural performance. Factors influencing the natural durability of wood include anatomical structure, density, chemical composition, and their respective contents. Wood-decay fungi are the primary agents responsible for wood decay, and their growth and reproduction depend on sufficient nutrient sources, moisture, suitable temperature, oxygen, and appropriate pH conditions (Guo *et al.* 2010). On the one hand, the inherent chemical components of wood, namely cellulose, hemicellulose, and lignin, provide abundant nutrients for decay fungi. On the other hand, the optimal growth temperature for decay fungi ranges from 25 to 30 °C, and the optimal moisture content for reproduction is between 30% and 150% (Schwarze and Spycher 2005; Chen 2019). Within this range, wood moisture content is positively correlated with decay rate (Yang *et al.* 2025). When environmental conditions such as temperature and humidity meet the growth requirements of fungi, the components of wood cell walls are metabolized and decomposed by fungi. This process ultimately leads to wood decay, which manifests as performance degradation, shortened service life, and reduced use value (Goodell *et al.* 2020).

The assessment of the decay status of wooden components in ancient Chinese buildings mostly relies on non-destructive testing (NDT) techniques such as stress wave, resistograph, and ultrasonic testing (Chang *et al.* 2022; Mvolo *et al.* 2022; Zhang *et al.* 2022; Bai *et al.* 2023). Although these methods comply with the principle of minimum intervention in heritage conservation, they are limited to macroscopic defect identification. They cannot detect early-stage deterioration at the microscale, nor can they fully reflect the impact of decay on the internal structure of wood. Therefore, it is urgent to investigate the decay changes of wood at the micro level by focusing on its microstructure and chemical composition.

In the field of wood microstructural analysis, various analytical techniques offer distinct advantages. Polarized light microscopy characterizes cellulose degradation *via* the birefringence of crystalline cellulose regions (Cui *et al.* 2016), while fluorescence microscopy assesses lignin concentration based on its inherent autofluorescence (He *et al.* 1999; Balzano *et al.* 2022). Safranin O is a basic dye that stains lignin in wood tissues red, enabling qualitative assessment of lignin content in wood cells. Methylene blue, also a basic dye, is adsorbed by amorphous cellulose and hemicellulose in wood tissues;

accordingly, methylene blue staining can be applied for the qualitative determination of amorphous cellulose and hemicellulose contents (Yu and Zhang 1989; Micco and Aronne 2007; Yang *et al.* 2026; Yang *et al.* 2020). In recent years, these micro-destructive testing techniques have been increasingly applied to assess the material condition of wooden components in historic buildings. Researchers have employed polarized light and fluorescence microscopy to quantify wood degradation (Gan *et al.* 2020; Yang *et al.* 2022; Li *et al.* 2019), and to establish decay grading criteria based on microstructural features (Cui et al. 2016; Yang *et al.* 2025).

This study examined wooden components from Traditional Dwelling No. 9, Dongmenli, Gulian Village using cross-validated polarized light microscopy, fluorescence microscopy, and histochemical staining to characterize chemical degradation across wood species, identify deterioration drivers, and propose tailored conservation and restoration strategies. The results are expected to provide theoretical references and technical solutions for the scientific protection of wooden cultural relic buildings in the Jinzhong region.

EXPERIMENTAL

Materials

Wood samples were collected from columns, beams, purlins, rafters, doors, and windows of Traditional Dwelling No. 9, East Gate Lane, Gulian Village, Qi County, Jinzhong City, Shanxi Province using an increment borer (Model 10-100-1027, Haglöf AB, Sweden) (Fig. 2).

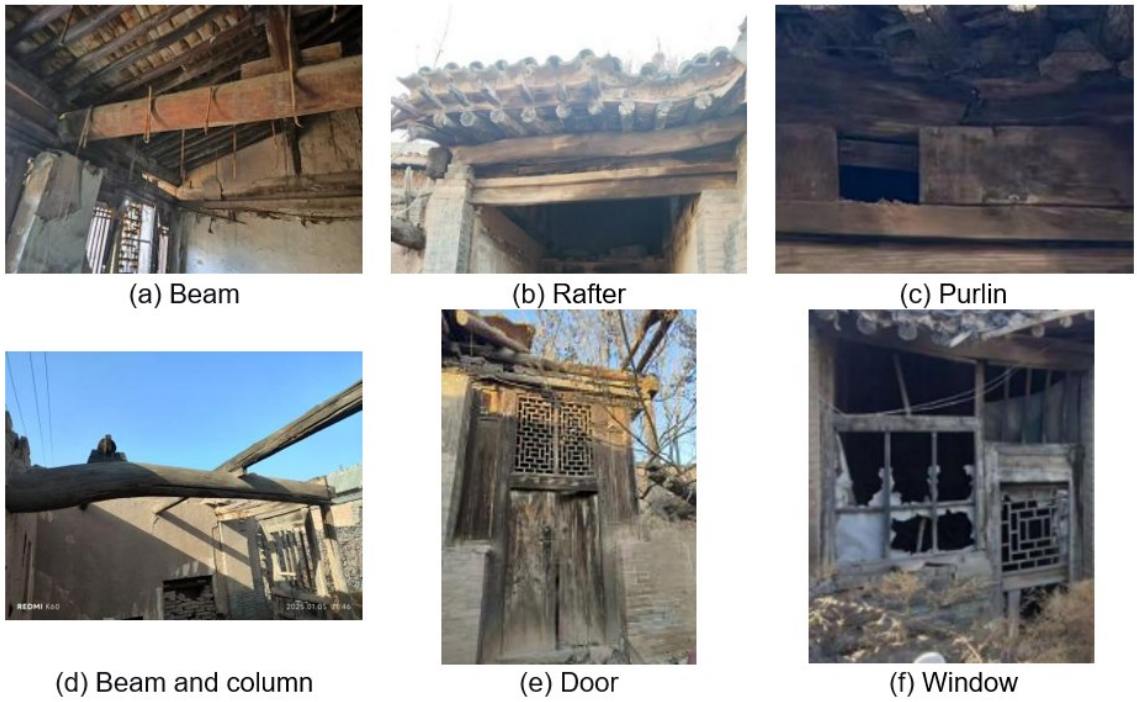

Fig. 2. Sampling locations of wooden components

Sampling sites were prioritized on high-deterioration-risk sites: column bases, wall-embedded column sections, timber ends, eaves purlins, and eaves rafter tips. The samples

included visibly decayed wood, insect-damaged wood, and sound wood with no apparent defects. These sampling sets can authentically reflect the material selection, service conditions, and diverse degradation patterns of the building's wooden components. All samples were taxonomically identified by the authors, and the wooden components belong to six wood taxa: *Larix* sect. *Multiseriales*, *Pinus tabulaeformis*, *Betula* spp., *Populus* spp., *Salix* sect. *Salix,* and *Ulmus* sect. *Madocarpus*. Detailed sampling locations and quantities are presented in Table 1.

Control woods were sourced from healthy standing trees of Chinese larch, Chinese pine, birch, poplar, and elm, all aged over 30 years.

Table 1. Sample Information of Wooden Components

Number	Location	Macroscopic Damage	Tree Species
No. 6	Rafter	Cracking, rafter tip decay	Chinese larch (*Larix*)
No. 7	Rafter	Cracking, rafter tip decay	
No. 9	Window	Cracking, deformation, and damage	
No. 8	Purlin	Slight cracking	Chinese pine (*Pinus tabulaeformis)*
No.12	Door	Cracking, deformation, and decay	
No. 18	Door	Cracking, deformation, and decay	
No. 4	Purlin	Cracking, decay	Birch (*Betula* spp.)
No. 5	Purlin	Cracking, decay	
No. 13	Beam	Distortion, shrinkage cracks	
No. 3	Wood column	Shrinkage cracks, decay	Poplar (*Populus* spp.)
No. 11	Door	Cracking, deformation, and decay	
No. 17	Rafter	Cracking, rafter tip decay	
No. 1	Beam	Distortion, shrinkage cracks	Elm (*Ulmus* sect. *Madocarpus)*
No. 2	Window	Cracking, deformation, and damage	Willow (*Salix* sect. *Salix)*
No. 10	Window	Cracking, deformation, and damage	
No. 14	Beam	Distortion, shrinkage cracks, and insect damage	
No. 15	Beam	Distortion, shrinkage cracks, and insect damage	
No. 16	Door	Cracking, deformation, and decay	

Staining Reagents

Safranin O was purchased from Phygene Biotechnology Co., Ltd., and methylene blue from Hunan BKMAM Holdings Co., Ltd. All staining reagents were of analytical grade and used without further purification.

Preparation and Histochemical Staining of Wooden Component Sections

The preparation procedure for wooden component sections was performed as described previously (Yang *et al.* 2024). (1) Sampling: Samples were cut into cubes of approximately 1 cm in size, ensuring that each transverse section contained at least one growth ring. (2) Softening: Wood samples were softened by boiling in water for 4 to 5 hours. (3) Sectioning: Treated specimens were sectioned using a Leica microtome (Model HistoCore AUTOCUT, Leica Biosystems, Germany) to obtain transverse, radial, and tangential sections with a thickness of 10 to 15 µm. (4) Staining: Sections were immersed in 3% safranin O aqueous solution and 0.1% methylene blue aqueous solution, respectively, for more than 2 hours. (5) Dehydration: Sections were dehydrated in a graded ethanol series

(50%, 75%, 95%, and 100%) for 10 min at each concentration. (6) Clearing: Sections were cleared in xylene solution for 3 to 5 min. (7) Mounting: Sections were mounted on glass slides using neutral balsam.

Observation of Wooden Component Sections under Polarized Light, Fluorescence, Methylene blue, and Safranin O Staining

Microstructural observations of the prepared wood sections were performed using an upright fluorescence microscope (Model ECLIPSE Ni-U, Nikon Corporation, Japan). Micrographs were obtained under polarized light, fluorescence, and after staining with methylene blue and safranin O, respectively.

Polarized light microscopy was used to qualitatively assess the degradation state of crystalline cellulose regions in wood cell walls based on the Birefringence Brightness of Crystalline Cellulose (BBCC). Higher brightness indicates higher cellulose content, while reduced brightness reflects cellulose degradation (Kanbayashi and Miyafuji 2016; Cui *et al.* 2016; Yang *et al.* 2025). Fluorescence microscopy with a blue excitation filter block (515 to 560 nm) was used to qualitatively determine lignin degradation in wood cell walls based on the Green Fluorescence Brightness of Lignin (GFBL). Higher GFBL corresponds to higher lignin density and concentration (Ma *et al.* 2011; Liu *et al.* 2017; Kiyoto *et al.* 2018; Yang *et al.* 2020; Martin and Lopez 2023; Ji *et al.* 2024).

Based on the principle that amorphous cellulose and hemicellulose can adsorb methylene blue, the distribution and content of these components within cell walls can be qualitatively assessed. A deeper blue color indicates higher contents of cellulose and hemicellulose (Yang *et al.* 2026; Toy *et al.* 2025). Safranin O staining stains lignin red, enabling qualitative evaluation of lignin distribution and content in cell walls (Criswell *et al.* 2025). Deeper red coloration indicates higher lignin concentration (Vazquez-Cooz *et al.* 2002; Guillermo *et al.* 2004; Ding 2010).

Wood degradation level was determined based on the BBCC as well as the GFBL. If these values are similar to those of the control wood, then it is defined as slight degradation. If they decrease by 33% to 50% compared to the control, then it is defined as medium degradation. If they decrease by more than 50% compared to the control, then it is defined as serious degradation (Ji *et al.* 2024; Yang *et al.* 2025).

By comprehensively comparing the BBCC, the GFBL, and the staining results of methylene blue and safranin O, the degradation degree of chemical components and the overall deterioration state of wooden components can be systematically evaluated.

RESULTS AND DISCUSSION

Chemical Degradation Analysis of Elm Wooden Components

The degradation characteristics of elm wooden components under bright-field light, polarized light and fluorescence are presented respectively in Figs. 3 a-c. Under bright-field illumination (Fig. 3 a), the cell walls of vessels, ground tissue fibers, and wood rays in Sample No. 1 remained intact with no visible damage. Under polarized light (Fig. 3 b), Sample No. 1 exhibited distinct BBCC. Its signal intensity was 15 to 30% lower than that of the control wood, indicating that a large proportion of crystalline cellulose was retained in the sample. Under green fluorescence (Fig. 3 c), the GFBL of Sample No. 1 was weak, measuring only 40 to 50% of that of sound wood. This indicates partial degradation of the aromatic ring structure of lignin in the sample.

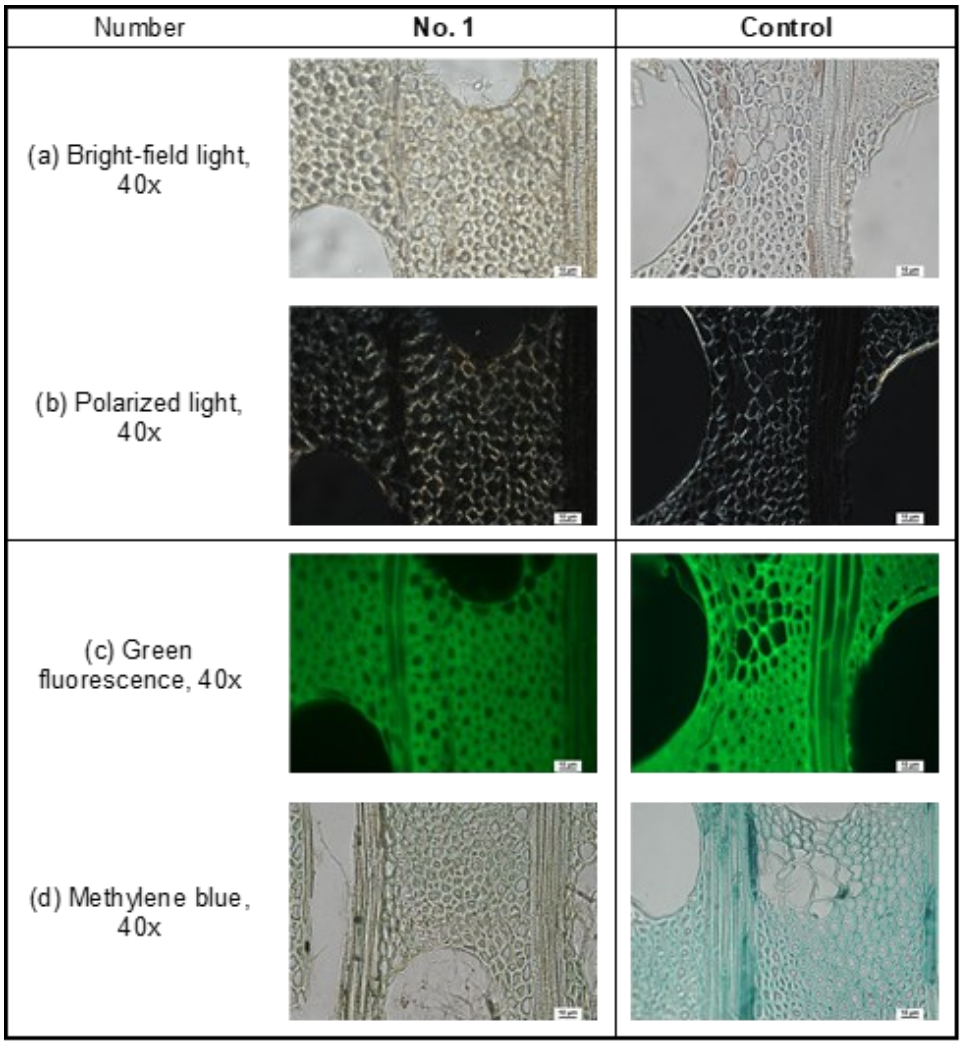

Fig. 3. Microscopic effects of elm wooden components under Bright-field light, Polarized light, Green fluorescence, Methylene blue, and Safranin O

Under methylene blue staining (Fig. 3 d), Sample No. 1 exhibits relatively distinct blue staining in the cell walls, indicating that partial hemicellulose and amorphous cellulose are retained in the sample. Under safranin O staining (Fig. 3 e), Sample No. 1 shows relatively pronounced red staining, suggesting a partial reduction in lignin content, which is broadly consistent with the fluorescence observations.

Integrated analysis of the microstructures of elm wooden components under bright-field illumination, polarized light, fluorescence, and histochemical staining (Fig. 3) reveals that Sample No. 1 undergoes slight cellulose degradation and moderate lignin degradation, with lignin degradation being more severe. It is concluded that the chemical components of Sample No. 11 are moderately degraded (Table S1).

Chemical Degradation Analysis of Poplar Wooden Components

The degradation characteristics of poplar wooden components under bright-field light, polarized light and fluorescence microscopy are shown respectively in Figs. 4 a-c. Under bright-field illumination (Fig. 4 a), the vessel cell walls of Sample No. 17 were severely damaged, and the ground tissue fibers and cell walls were slightly damaged.

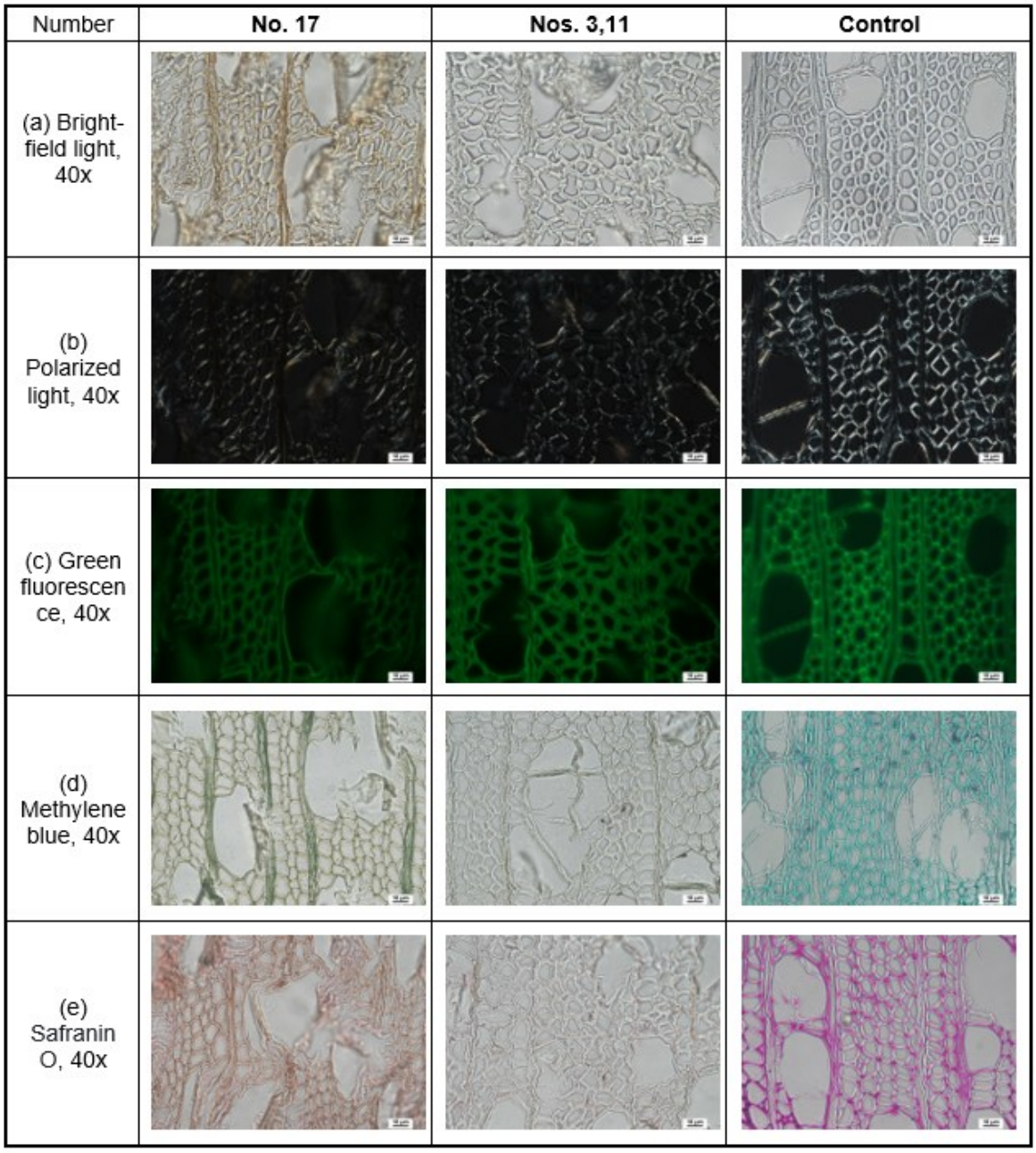

Fig. 4. Microscopic effects of poplar wooden components under Bright-field light, Polarized light, Green fluorescence, Methylene blue, and Safranin O

The vessel cell walls of Samples Nos. 3 and 11 were slightly damaged, while their wood fiber cell walls remained largely intact. Under polarized light (Fig. 4 b), the BBCC of Sample No. 17 was very weak, with a reduction of 60 to 80% compared with the control wood, indicating severe reduction of crystalline cellulose content in Sample No. 17. The BBCC of Samples Nos. 3 and 11 was distinct but decreased by 45 to 50% relative to the control wood, suggesting partial degradation of crystalline cellulose in these two samples. Under fluorescence, the GFBL of Sample No. 17 was extremely weak, with a reduction of 70 to 90% compared with the control wood, indicating extensive degradation of the aromatic ring structure of lignin. Under green fluorescence (Fig. 4 c), the GFBL of Samples Nos. 3 and 11 were relatively distinct but decreased by 50 to 70% compared with the control wood, indicating moderate degradation of lignin. Under methylene blue staining (Fig. 4 d), cell walls of Samples Nos. 3, 11 and 17 all exhibit faint blue staining. However, Sample No. 17 shows deeper blue intensity than Samples Nos. 3 and 11. When combined with polarized light results, this indicates that crystalline cellulose in Sample No. 17 has undergone extensive degradation and been converted into a certain amount of amorphous cellulose. Under safranin O staining (Fig. 4 e), red staining is faint across all three samples, but the red intensity in cell walls of Samples Nos. 3 and 11 is overall stronger than that of Sample No. 17. This pattern is broadly consistent with the fluorescence observations.

Integrated analysis of microstructures of poplar wooden components under bright-field illumination, polarized light, fluorescence and histochemical staining (Fig. 4) reveals that both cellulose and lignin in Sample No. 17 were severely degraded, with lignin degradation being more severe than cellulose degradation. For Samples Nos. 3 and 11, cellulose had undergone moderate degradation while lignin was severely degraded. It is concluded that Sample No. 17 is severely degraded, and Samples Nos. 3 and 11 were moderately degraded (Table S1).

Chemical Degradation Analysis of Willow Wooden Components

Degradation characteristics of willow wooden components under bright-field light, polarized light and fluorescence microscopy are presented respectively in Figs. 5 a-c. Under bright-field illumination (Fig. 5 a), the vessel cell walls of Samples Nos. 15 and 16 were severely damaged, and their wood fiber cell walls were slightly damaged. The vessel cell walls of Sample No. 14 were slightly damaged, while its wood fiber cell walls remained largely intact. All cell walls of Samples Nos. 2 and 10 remained essentially intact. Under polarized light (Fig. 5 b), the BBCC of Samples Nos. 15 and 16 were extremely weak, with a reduction of more than 90% compared with the control wood, indicating almost complete degradation of crystalline cellulose in these samples. The BBCC of Sample No. 14 was relatively distinct but decreased by 50% to 70% relative to the control wood, suggesting moderate reduction of crystalline cellulose content. The BBCC of Samples Nos. 2 and 10 were distinct but decreased by 30% to 40% compared with the control wood, indicating that a large proportion of crystalline cellulose was retained. Under green fluorescence (Fig. 5 c), the GFBL of Samples Nos. 15 and 16 were extremely weak, with a reduction of 85% to 95% compared with the control wood, indicating severe degradation of the aromatic ring structure of lignin. The GFBL of Sample No. 14 was weak but decreased by 70% to 80% compared with the control wood, indicating relatively severe degradation of the aromatic ring structure of lignin. The GFBL of Samples Nos. 2 and 10 were distinct but decreased by 35% to 45% compared with the control wood, indicating partial degradation of the aromatic ring structure of lignin.

Under methylene blue staining (Fig. 5 d), the cell walls of Samples Nos. 14-16 show faint blue staining intensity, indicating a severe reduction in amorphous cellulose and hemicellulose contents. In contrast, Samples Nos. 2 and 10 exhibit distinct blue staining intensity, suggesting only a minor decrease in these components. Under safranin O staining (Fig. 5 e), the cell walls of Samples Nos. 14-16 display faint red staining intensity, while those of Samples Nos. 2 and 10 show relatively pronounced red staining. This pattern is broadly consistent with the fluorescence observations.

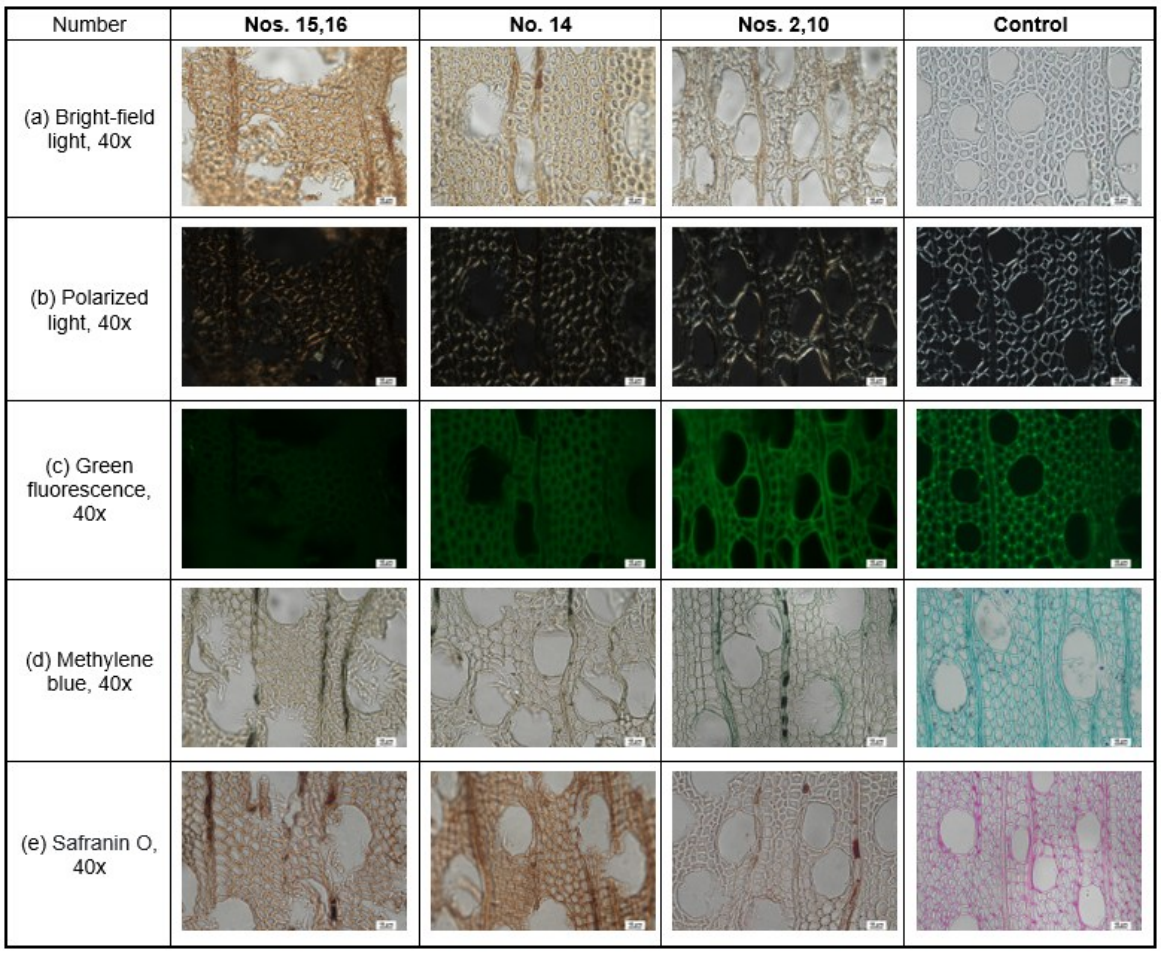

Fig. 5. Microscopic effects of willow wooden components under Bright-field light, Polarized light, Green fluorescence, Methylene blue, and Safranin O

Integrated analysis of the microstructures of willow wooden components under bright-field illumination, polarized light, fluorescence, and histochemical staining (Fig. 5) reveals that both cellulose and lignin are severely degraded in Samples Nos. 14 to 16, with Sample No. 14 exhibiting more severe lignin degradation than cellulose degradation. Samples Nos. 2 and 10 undergo moderate degradation of both components. It can be concluded that Samples Nos. 14 to 16 are severely degraded, while Samples Nos. 2 and 10 are moderately degraded (Table S1).

Chemical Degradation Analysis of Birch Wooden Components

Degradation characteristics of birch wooden components under bright-field light, polarized light and fluorescence microscopy are shown respectively in Figs. 6 a-c.

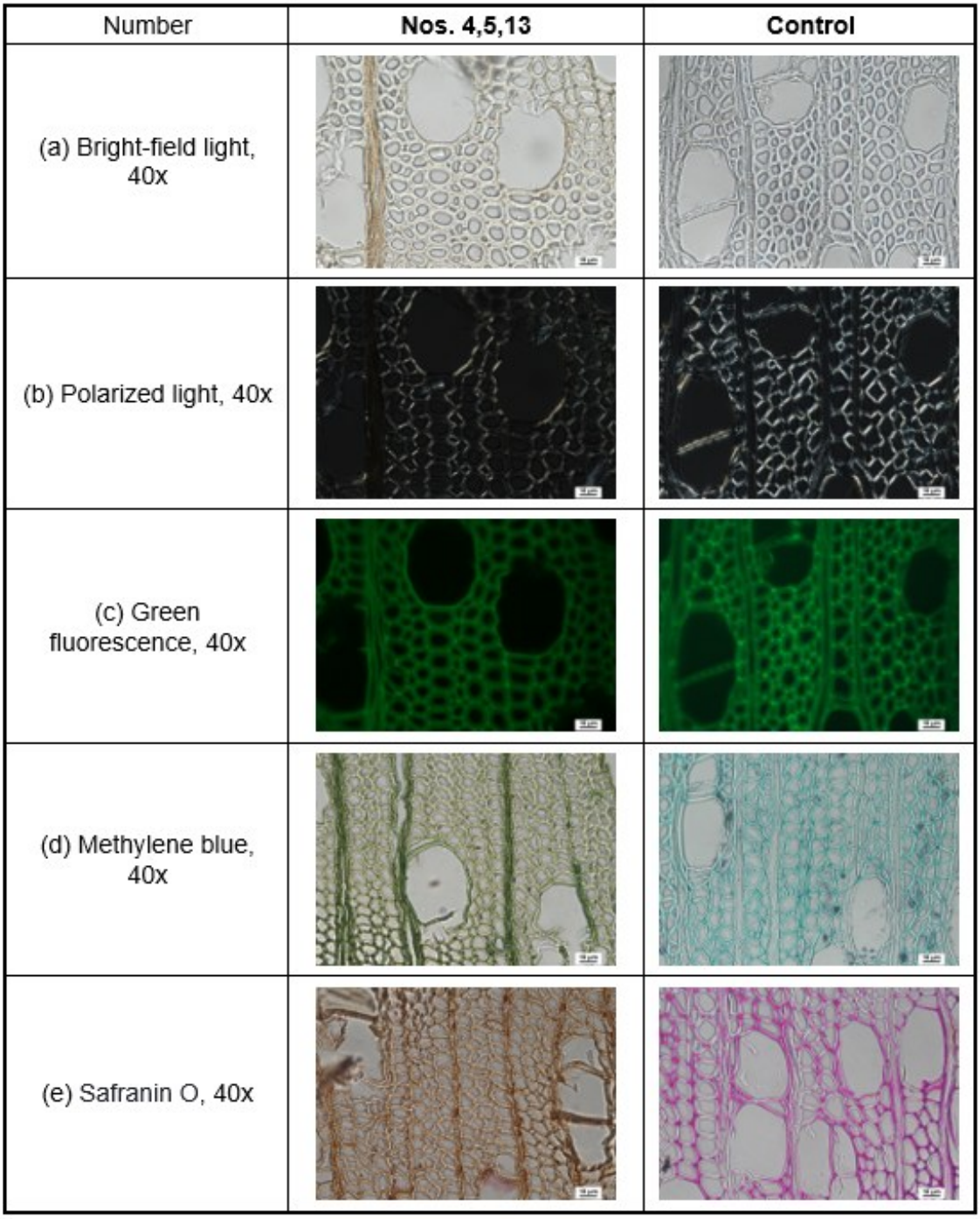

Fig. 6. Microscopic effects of birch wooden components under Bright-field light, Polarized light, Green fluorescence, Methylene blue, and Safranin O

Under bright-field illumination (Fig. 6 a), the vessel cell walls of Samples Nos. 4, 5, and 13 were slightly damaged, while the ground tissue fibers and cell walls remained relatively intact. Under polarized light (Fig. 6 b), the BBCC of Samples Nos. 4, 5, and 13 were distinct, with a reduction of 35% to 50% compared with the control wood, indicating a certain degree of reduction in crystalline cellulose content. Under green fluorescence (Fig. 6 c), the GFBL of Samples Nos. 4, 5, and 13 were relatively distinct, with a reduction of 40% to 50% compared with the control wood, indicating partial degradation of the aromatic ring structure of lignin.

Under methylene blue staining (Fig. 6 d), Samples Nos. 4, 5 and 13 show relatively distinct blue staining intensity in cell walls, indicating that a certain amount of amorphous cellulose and hemicellulose remains in the wooden components. Under safranin O staining (Fig. 6 e), the corresponding red staining confirms residual lignin in the components, which is broadly consistent with the fluorescence observations.

Integrated analysis of the microstructures of birch wooden components under bright-field illumination, polarized light, fluorescence and histochemical staining (Fig. 6) reveals that both cellulose and lignin in Samples Nos. 4, 5 and 13 undergo moderate degradation. It can be concluded that Samples Nos. 4, 5 and 13 are moderately degraded (Tab. 2).

Comprehensive analysis of the microstructural images of birch wooden components under bright field, polarized light, fluorescence, methylene blue staining, and safranin O staining (Fig. 6) leads to the conclusion that Samples Nos. 4, 5, and 13 suffered moderate degradation .

Chemical Degradation Analysis of Chinese Larch Wooden Components

Degradation characteristics of Chinese larch wooden components under bright-field light, polarized light and fluorescence microscopy are presented respectively in Fig. 7 a-c. Under bright-field illumination (Fig. 7 a), a small portion of latewood cell walls in Samples Nos. 6 and 7 were fractured, while their vessel cell walls remained intact. Both latewood and vessel cell walls in Sample No. 9 remained intact. Under polarized light (Fig. 7 b), the BBCC of Samples Nos. 6, 7, and 9 were distinct, with a reduction of 35% to 50% compared with the control wood, indicating a certain degree of reduction in crystalline cellulose content. Among them, Sample No. 9 exhibits higher polarized light intensity than Samples Nos. 6 and 7. Under green fluorescence (Fig. 7 c), the GFBL of Samples Nos. 6, 7, and 9 were relatively distinct, with a reduction of 30% to 40% compared with the control wood, indicating partial degradation of the aromatic ring structure of lignin.

Under methylene blue staining (Fig. 7 d), Samples Nos. 6 and 7 exhibit stronger blue staining intensity in cell walls than Sample No. 9, indicating extensive degradation of crystalline cellulose into amorphous cellulose in these samples. This is consistent with the polarized light observations. Under safranin O staining (Fig. 7 e), Samples Nos. 6, 7 and 9 show relatively pronounced red staining in cell walls, which is broadly consistent with the fluorescence observations.

Integrated analysis of the microstructures of Chinese larch wooden components under bright-field illumination, polarized light, fluorescence, and histochemical staining (Fig. 7) reveals that both cellulose and lignin in Samples Nos. 6, 7 and 9 undergo moderate degradation. It can be concluded that Samples Nos. 6, 7 and 9 are moderately degraded (Table S1).

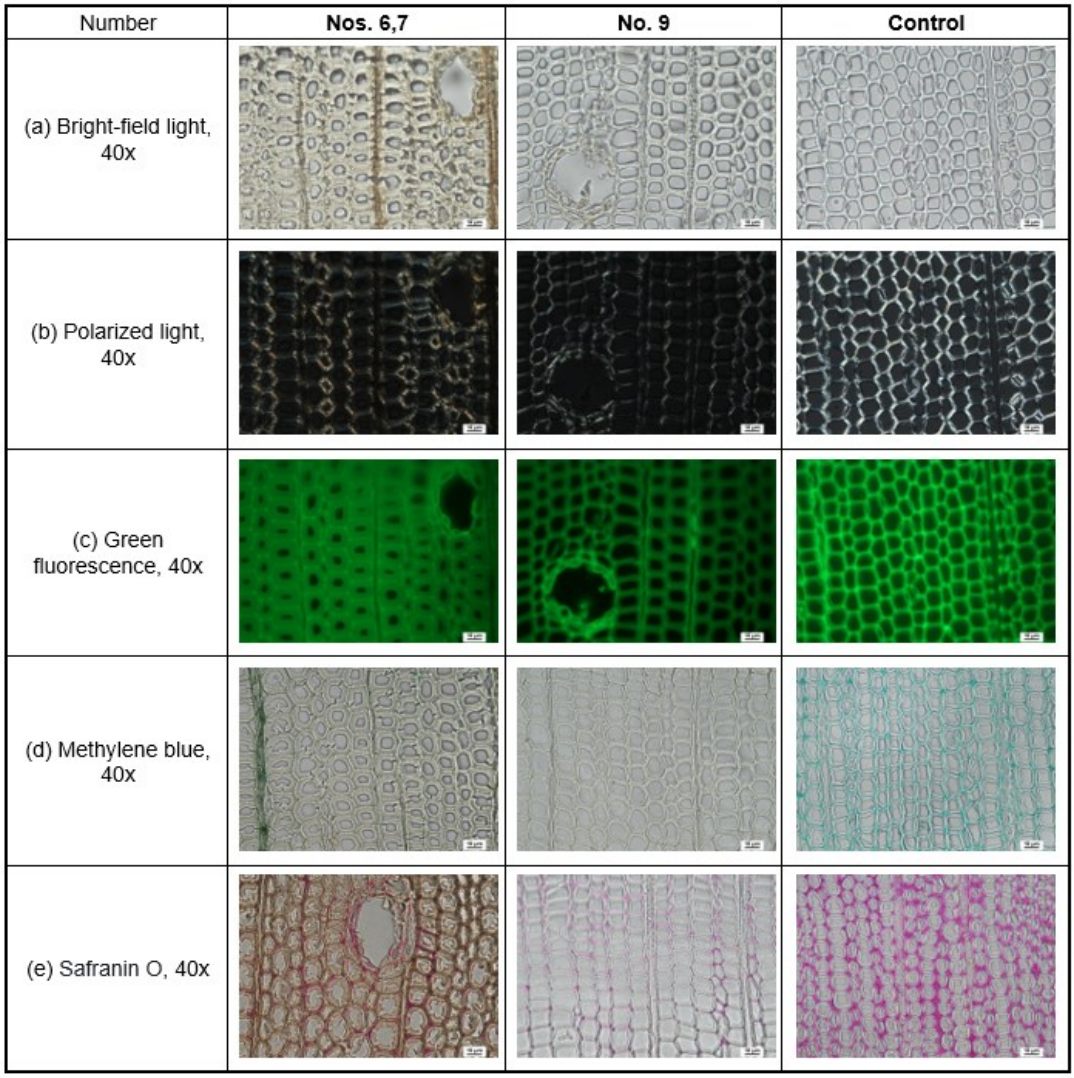

Fig. 7. Microscopic effects of Chinese larch wooden components under Bright-field light, Polarized light, Green fluorescence, Methylene blue, and Safranin O

Chemical Degradation Analysis of Chinese Pine Wooden Components

Degradation characteristics of Chinese pine wooden components under polarized light and fluorescence microscopy are presented respectively in Figs. 8 a-c. Under bright-field illumination (Fig. 8 a), the latewood cell walls of Samples Nos. 8 and 12 were slightly damaged. The latewood cell walls of Sample No. 18 remained largely intact. Under polarized light (Fig. 8 b), the BBCC of Samples Nos. 8 and 12 were relatively distinct, with a reduction of 45% to 60% compared with the control wood, indicating a greater degree of reduction in crystalline cellulose content. The BBCC of Sample No. 18 was distinct but decreased by 5% to 15% relative to the control wood, suggesting mild degradation of crystalline cellulose. Under green fluorescence (Fig. 8 c), the GFBL of Samples Nos. 8 and 12 were distinct, with a reduction of 30% to 45% compared with the control wood, indicating partial degradation of the aromatic ring structure of lignin. The GFBL of Sample No. 18 was weak but decreased by 50% to 60% compared with the control wood, indicating extensive degradation of the aromatic ring structure of lignin.

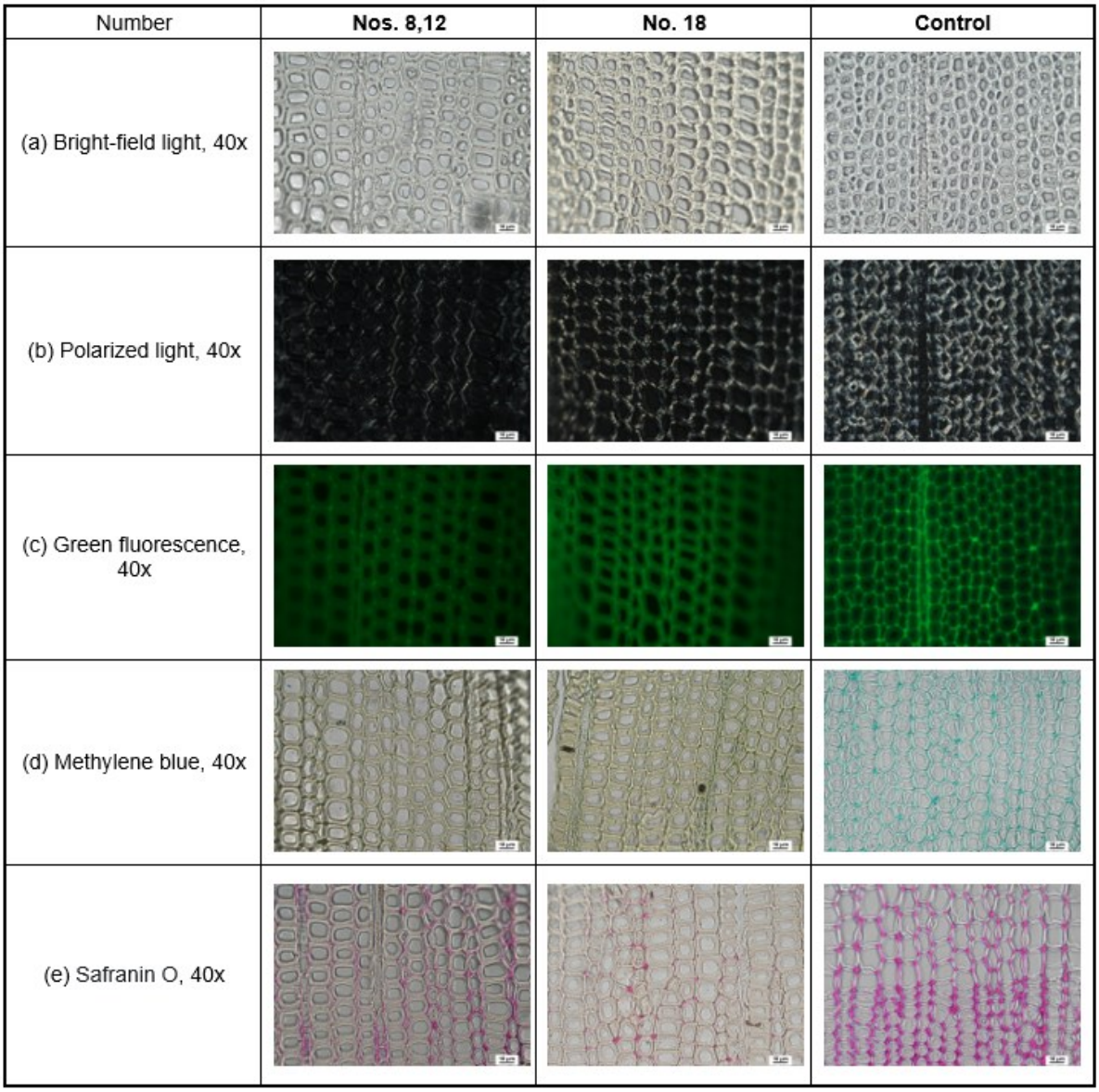

Fig. 8. Microscopic effects of Chinese pine wooden components under Bright-field light, Polarized light, Green fluorescence, Methylene blue, and Safranin O

Under methylene blue staining (Fig. 8 d), Samples Nos. 8, 12 and 18 all show relatively distinct blue staining in cell walls, with Sample No. 18 exhibiting deeper blue intensity than Samples Nos. 8 and 12, indicating higher contents of amorphous cellulose and hemicellulose in Sample No. 18. Under safranin O staining (Fig. 8 e), all three samples display relatively pronounced red staining in cell walls, which is broadly consistent with the fluorescence observations.

Integrated analysis of the microstructures of Chinese pine wooden components under bright-field illumination, polarized light, fluorescence and histochemical staining (Fig. 8) reveals that both cellulose and lignin in Samples Nos. 8 and 12 had undergone moderate degradation. Sample No. 18 exhibits slight cellulose degradation and moderate lignin degradation, with lignin degradation being markedly more severe than cellulose degradation. It can be concluded that Samples Nos. 8, 12 and 18 are moderately degraded (Table S1).

Causes of Deterioration of Wooden Components

Inherent Properties of Wood

Among softwoods, Chinese larch has strong natural decay resistance (Cheng *et al.* 1992; Ma *et al.* 2011). However, it is light and soft in texture with low strength, making it suitable for non-load-bearing components such as doors, windows, furniture, and floors. Chinese pine is relatively hard and heavy with high strength. It is rich in resin and has good moisture and decay resistance, making it an excellent material for core load-bearing components such as beams and columns. Nevertheless, it has weak termite resistance. The study found obvious insect holes in Chinese pine wooden components of the residential building (Fig. 9a). Some rafter and purlin components made of Chinese larch and Chinese pine developed distinct helical cracks under long-term loading (Figs. 9b-c). Among hardwoods, elm is hard with high strength, making it an ideal material for load-bearing structures in ancient buildings. In contrast, poplar and willow have lower density and strength, and their natural decay and insect resistance are weaker than those of elm (Fang *et al.* 2024). Obvious insect holes were also observed in poplar and willow wooden components of the building (Figs. 9d-f).

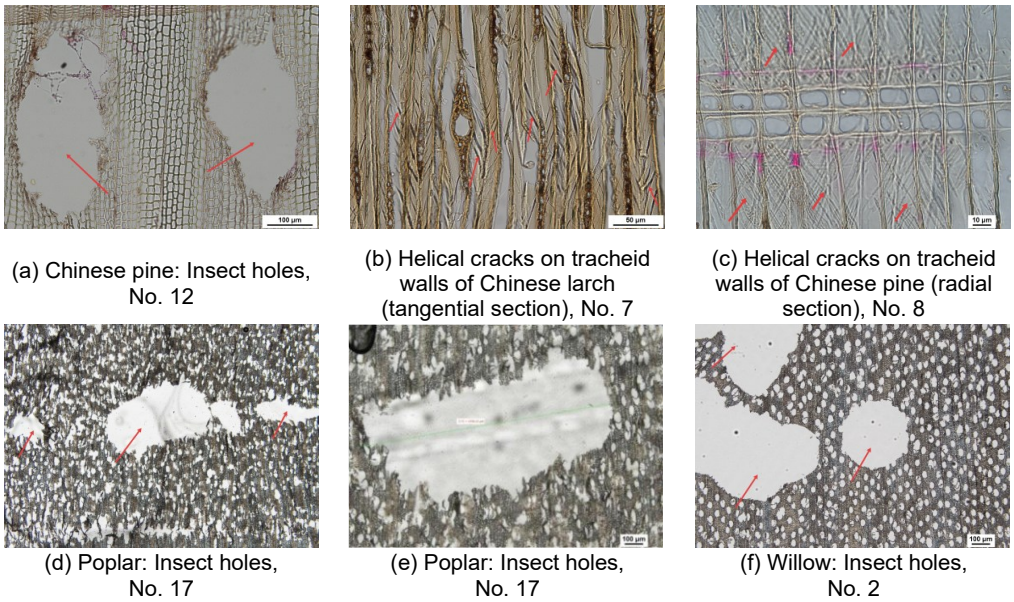

(a) Chinese pine: Insect holes, No. 12

(b) Helical cracks on tracheid walls of Chinese larch (tangential section), No. 7

(c) Helical cracks on tracheid walls of Chinese pine (radial section), No. 8

(d) Poplar: Insect holes, No. 17

(e) Poplar: Insect holes, No. 17

(f) Willow: Insect holes, No. 2

Fig. 9. Microstructures of the wooden components Nos. 2, 6, 8, 17 under bright-field light

Chemical component degradation is the fundamental cause of macroscopic property changes and microstructural damage in wood. Studies by Curling *et al.* (2002) and Ge *et al.* (2017) demonstrate that the initial reduction in wood strength (bending strength and impact toughness) is primarily attributed to the scission and degradation of hemicellulose side chains and backbones, while the subsequent decline in mechanical properties (compressive strength parallel to grain, modulus of elasticity, and hardness) is closely associated with cellulose depolymerization. Lignin degradation is another key factor driving wood mass loss and reductions in strength and hardness.

Different wood-decay fungi exhibit distinct substrate preferences: white-rot fungi preferentially degrade lignin while retaining most cellulose; brown-rot fungi primarily decompose cellulose and hemicellulose, leaving a high residual lignin content (Guo *et al.* 2010; Goodell *et al.* 2017; Irbe *et al.* 2011; Bari *et al.* 2015); soft-rot fungi can break down

all three components, but have limited lignin-degrading capacity, with degradation focused mainly on cellulose and hemicellulose (Guo *et al.* 2010). Consistent with the degradation patterns observed in this study, lignin degradation in Nos. 1 and 18 was far more severe than cellulose degradation (Tab. 2), suggesting that these two wooden components (No. 1: elm; No. 18: Chinese pine) were attacked by white-rot fungi. For all other samples, the degrees of lignin and cellulose degradation were comparable (Tab. 2), indicating that fungal decay in the remaining wooden components of Gulian Village has been dominated by soft-rot fungi.

External Environmental Impacts

Qi County in Shanxi Province has a warm temperate continental climate with four distinct seasons and a large annual temperature range. The annual average temperature is 9.9 °C, and the annual precipitation is approximately 500 mm. It is characterized by dry springs and autumns, hot and humid summers, and sunny and dry winters with abundant sunshine. Previous studies have shown that wood deterioration in ancient buildings in Shanxi Province is directly related to oxidative degradation and the intrusion of acidic substances from acid rain and air pollution (Li and Meng 2024). Wooden components of residential buildings in Gulian Village have been subjected to centuries of environmental stress. Long-term exposure to alternating wet and dry conditions and intense solar radiation cycles has created the necessary conditions for fungal colonization and biodegradation through periodic fluctuations in wood moisture content and the inherent chemical composition of wood.

(a) Decay and cracking of rafter tips

(b) Distortion of beam frames and damage to the waterproof layer

(c) Roof collapse and vegetation growth; Severe decay of window

(d) Severe decay and insect infestation of doors

Fig. 10. Decay-prone areas of wooden components in Traditional Dwelling No. 9, East Gate Lane, Gulian Village

Directly exposed components such as column bases, flying rafter tips, purlins, and rafters in damaged roof areas, doors and windows, as well as concealed columns within walls, are high-risk areas for decay due to persistently high moisture content (Fig. 10). In this study, rafter components (Nos. 6, 7, 17) and door and window components (Nos. 2, 9 to 12, 16, 18) were all located in these high-risk areas. Affected by the combined effects of rainwater infiltration and ultraviolet radiation, these components experienced large fluctuations in moisture content, and their deterioration degree was significantly higher than that of components in concealed locations.

CONCLUSIONS

1. All six types of wooden components, including elm, poplar, willow, birch, Chinese larch, and Chinese pine, exhibited moderate to severe chemical degradation. Elm components were mainly attacked by white-rot fungi, while the other wood species were predominantly affected by soft-rot fungi. Poplar and willow were found to be more susceptible to insect damage.
2. The deterioration of wooden components results from the synergistic effect of internal and external factors. The internal factor is the difference in natural decay resistance among tree species, with hardwoods showing overall more severe deterioration than softwoods. The external factors include rainwater erosion, intense ultraviolet radiation, structural damage, microbial infection, and temperature and humidity cycles. Components with high exposure and high moisture content showed more intense degradation.
3. Based on the microscopic degradation characteristics and underlying deterioration mechanisms, the following conservation recommendations are proposed: preventive anti-decay and anti-insect treatments for sound wooden components; timely repair of the roof and drainage systems to block water ingress; enhanced moisture proofing, light shielding, and ventilation at high-risk sites such as column bases and eave rafter ends; and crack repair with breathable materials to prevent moisture retention and mitigate fungal decay attack.

This study has several limitations that require further refinement. With samples confined to a single traditional dwelling, the generalizability of the findings is constrained. Fungal decay types were identified *via* indirect inference, without direct supporting microbiological evidence. Degradation assessment relied on semi-quantitative estimation, with scope for improved quantitative accuracy. The proposed conservation strategies remain largely principled frameworks and need further elaboration to enhance practical applicability.

ACKNOWLEDGMENTS

This work was supported by the Natural Science Foundation Project of Henan Province [252300420061], the Key Research and Development and Promotion Project of Henan Province [242102320293], the Key Research Project of University in Henan Province [24A560017], and the Research Fund Project for College Students of Nanyang Institute of Technology [NGDJ-2025-88].

Conflict of Interest

The authors have no relevant financial or non-financial interests to disclose.

Use of Generative AI

The authors used the Doubao AI Assistant solely for language polishing and stylistic refinement of the manuscript. No generative AI tools were used for data analysis, interpretation, image or figure preparation, or the generation of scientific content.

REFERENCES CITED

Bai, X.-B., Wu, J.-S., Yang, N., and Liang, N.-B. (2023). "Research on non-destructive testing technology for properties of ancient larch wood materials in Shanxi," *Journal of Taiyuan University of Technology* 54(6), 1101-1108. https://doi.org/10.16355/j.tyut.1007-9432.2023.06.018

Balzano, A., Čufar, K., and De Micco, V. (2022). "Cell-wall fluorescence highlights the phases of xylogenesis," *IAWA Journal* 43(1), 80-91. https://doi.org/10.1163/22941932-bja10080

Bari, E., Taghiyari, H.-R., Mohebbi, B., Clausen, C.A., Schmidt, O., Tajick Ghanbary, M.-A., and Vaseghi, M.-J. (2015). "Mechanical properties and chemical composition of beech wood exposed for 30 and 120 days to white-rot fungi," *Holzforschung* 69, 587-593. https://doi.org/10.1515/hf-2014-0057

Chang, L.-H., Qian, W., Chang, H., Li, X., Dai, J., and Chang, X.-H. (2002). "Detection of internal voids in wooden components by stress wave," *Wood Science and Technology* 36(4), 70-76.

Chen, K.-Y. (2019). *A Study on Wood Decay and Drying Shrinkage Cracks of Wooden Components*, Ph.D. dissertation, Southeast University. https://doi.org/10.27014/d.cnki.gdnau.2019.004080

Cheng, J.-Q., Yang, J.-J., and Liu, P. (1992). *A Record of Chinese Timber*, China Forestry Publishing House, Beijing, China.

Criswell, S., Gaylord, B., and Pitzer, C. R. (2024). "Histological methods for plant tissues," *Journal of Histotechnology* 48(1), 1-10. https://doi.org/10.1080/01478885.2024.2397989

Cui, X.-J., Qiu, J., and Gao, J.-R. (2016). "Determination of decay grades and analysis of reinforcement degree of ancient wood using fluorescence polarization technology," *Sciences of Conservation and Archaeology* 28(4), 48-53.

Curling, S. F., Clausen, C. A., and Winandy, J. E. (2002). "Relationships between mechanical properties, weight loss, and chemical composition of wood during incipient brown-rot decay," *For. Prod. J.* 52, 34-39.

Fang, X., Zhang, J.-P., Li, J.-X., Xiong, Y.-X., Yang, S.-Y., and Ma, X.-X. (2024). "A study on decay resistance and preservative treatability of three types of broad-leaved tree species commonly used in ancient buildings," *Wood Science and Technology* 38(2), 29-35.

Gan, C.-T., He, H.-S., Li, J., and Guo, M.-L. (2020). "Polarized fluorescence and infrared spectroscopy analysis of degradation degree of four types of fungal-patterned wood," *Journal of Southwest Forestry University (Natural Sciences)* 40(2), 155-160.

Ge, X.-W., Wang, L.-H., Hou, J.-J., Rong, B.-B., Yue, X.-Q., and Zhang, S.-M. (2017). "The effects of brown-rot decay on select wood properties of poplar (*Populus cathayana* Rehd.) and its mechanism of action," *Holzforschung* 71(4), 355-362. https://doi.org/10.1515/hf-2016-0150

Goodell, B., Zhu, Y., Kim, S., Kafle, K., Eastwood, D., Daniel, G., Jellison, J., Yoshida, M., Groom, L., and Pingali, S.-V. (2017). "Modification of the nanostructure of lignocellulose cell walls via a non-enzymatic lignocellulose deconstruction system in brown rot wood-decay fungi," *Biotechnol. Biofuels* 10, article 179. https://doi.org/10.1186/s13068-017-0865-2

Goodell, B., Winandy, J., and Morrell, J.-J. (2020). "Fungal degradation of wood: Emerging data, new insights and changing perceptions," *Coatings* 10(12), article

1210. https://doi.org/10.3390/coatings10121210
Guillermo, A., Shirley, A.-O., and Frank, W.-E. (2004). "Fluorescence shell: A novel view of sclereid morphology with the confocal laser scanning microscope," *Microscopy Research and Technique* 63(5), 282-288. https://doi.org/10.1002/jemt.20043
Guo, M.-L., Lan, H.-F., and Qiu, J. (2010). *Wood Decay and Maintenance*, China Metrology Press, Beijing, China.
He, X.-Q., Li, S.-W., Hu, Y.-X., and Lin, J.-X. (1999). "Microspectrofluorometric analysis of autofluorescence in the cell walls of *Phyllostachys pubescens* culm," *Acta Botanica Sinica* 1999(7), 38-41.
Irbe, I., Andersone, I., Andersons, B., Noldt, G., Dizhbite, T., Kurnosova, N., Nuopponen, M., and Stewart, D. (2011). "Characterisation of the initial degradation stage of Scots pine (*Pinus sylvestris* L.) sapwood after attack by brown-rot fungus *Coniophora puteana*," *Biodegradation* 22(4), 719-728. https://doi.org/10.1007/s10532-010-9449-6
Ji, H.-D., Yang, Y., Zhang, H., Li, B., and Cheng, L.-L. (2024). "Decay level classification of wooden components in Tingbao Yang's former residence utilizing polarization and fluorescence effects," *BioResources* 19(3), 4087-4103. https://doi.org/10.15376/biores.19.3.4087-4103
Kanbayashi, T., and Miyafuji, H. (2016). "Effect of ionic liquid treatment on the ultrastructural and topochemical features of compression wood in Japanese cedar (*Cryptomeria japonica*)," *Scientific Reports* 6(1), article 30147. https://doi.org/10.1038/srep30147
Kiyoto, S., Yoshinaga, A., Fernandez-Tendero, E., Day, A., Chabbert, B., and Takabe, K. (2018). "Distribution of lignin, hemicellulose, and arabinogalactan protein in hemp phloem fibers," *Microscopy and Microanalysis* 24(4), 442-452. https://doi.org/10.1017/S1431927618012448
Li, Y.-L., Wang, Y., and Hu, X.-J. (2024). "Protecting traditional villages and safeguarding the continuity of nostalgia," *Guangming Daily* (7). https://doi.org/10.28273/n.cnki.ngmrb.2024.005445
Li, W.-J. (2017). *A Study on the Settlement Pattern and Residential Architecture of Gulian Village in Qi County, Shanxi Province*, Master's Thesis, Taiyuan University of Technology.
Li, X., Fu, X.-H., Zhang, W.-B., Zhang, H.-J., Liu, H.-C., Wang, D.-Y., and Lu, W. (2019). "A study on material deterioration of wooden components in Changchun Palace of the Imperial Palace," *Sciences of Conservation and Archaeology* 31(1), 58-64. https://doi.org/10.16334/j.cnki.cn31-1652/k.2019.01.007
Liu, C.-W., Su, M.-L., Zhou, X.-W., Zhao, R.-J., Lu, J.-X., and Wang, Y.-R. (2017). "Analysis of content and distribution of lignin in cell wall of transgenic poplar with Fourier infrared spectrum (FTIR) and confocal laser scanning microscopy (CLSM)," *Spectroscopy and Spectral Analysis* 37(11), 3404-3408. https://doi.org/10.3964/j.issn.1000-0593(2017)11-3404-05
Li, Q.-L., and Meng, X.-J. (2024). "Study on and evaluation of deterioration of ancient wood in Maiden's Palace of Jinci based on XPS testing," *Museum* (6), 121-127.
Ma, X.-X., Jiang, M.-L., and Li, Z.-Q. (2011). *Wood Biodegradation and Protection*, China Forestry Publishing House, Beijing, China.
Micco, V.-D., and Aronne, G. (2007). "Combined histochemistry and autofluorescence for identifying lignin distribution in cell walls," *Biotechnic & Histochemistry* 82(4), 209-216. https://doi.org/10.1080/10520290701713981

Mvolo, C.-S., Stewart, J.-D., and Koubaa, A. (2022). "Comparison between static modulus of elasticity, non-destructive testing moduli of elasticity and stress-wave speed in white spruce and lodgepole pine wood," *Wood Material Science and Engineering* 17(5), 345-355. https://doi.org/10.1080/17480272.2021.1871949

Schwarze, F.-W.-M.-R., and Spycher, M. (2005). "Resistance of thermo-hygro-mechanically densified wood to colonisation and degradation by brown-rot fungi," *Holzforschung* 59(3), 358-363. https://doi.org/10.1515/HF.2005.059

Toy, M., Recepoğlu, Y. K., and Arar, Ö. (2025). "Sulfonated cellulose: A strategy for effective methylene blue sequestration," *ACS Omega* 10(8), 8696-8708. https://doi.org/10.1021/acsomega.5c00179

Yang, Y., He, Y.-M., Han, L., Wang, A.-F., Wang, W., Zhao, R., and Li, B. (2020). "Application of histochemical stains for rapid qualitative analysis of the lignin content in multiple wood species," *BioResources* 15(2), 3524-3533. https://doi.org/10.15376/biores.15.2.3524-3533

Yang, Y., Sun, H., Li, B., Han, L., Wang, A.-F., Wang, W., He, Y.-M., and Zhao, R. (2022). "Study on the identification and the extent of decay of the wooden components in the Xichuan Guild Hall ancient architectures," *International J. Architec. Heritage* 16(3), 405-414. https://doi.org/10.1080/15583058.2020.1786190

Yang, Y., Ji, H.-D., Li, B., and Liu, Y.-F. (2024). "Identification of the wood species and relationship between the wood species selection and the occurrence of biological diseases in wooden components within ancient wooden-structure building of Songyun Temple," *International Journal of Architectural Heritage* 19(9), 1870-1882. https://doi.org/10.1080/15583058.2024.2377296

Yang, Y., Li, B., and Ji, H.-D. (2025). *Theory and Practice of Renovation, Protection and Design of Ancient Architecture*, Chemical Industry Press, Beijing, China.

Yang, B., Chen, Z. Y., Ran, J. H., Yan, C., and Guo, Y. (2026). "Adsorption of methylene blue by cellulose/carboxymethyl chitosan composite aerogel," *Chemistry & Bioengineering* 43(6), 16-22. https://doi.org/10.3969/j.issn.1672-5425.2026.06.003

Yu, B. S., and Y. Zhang. (1989). *Biological Microscopic Techniques*, Beijing Agricultural University Press, Beijing, China.

Zhang, D., Yu, Y.-Z., Guan, C., Wang, H., Zhang, H.-J., and Xin, Z.-B. (2021). "Non-destructive testing study on the defect status of wooden columns in the wall of the Yangxin Hall of the Forbidden City," *J. Beijing Forestry University* 43(5), 127-139.

Article submitted: April 29, 2026; Peer review completed: July 4, 2026; Revised version received: July 7, 2026; Accepted: July 21, 2026; Published: August 4, 2026.
DOI: 10.15376/biores.21.4.9351-9372

APPENDIX
Supplementary Information

Table S1. Summary of Chemical Degradation Characteristics and Main Deterioration Drivers for Wooden Component Samples from Traditional Dwelling No. 9, Gulian Village

Sample Num.	Species	Component type	Exposure condition	BBCC reduction	GFBL reduction	Cellulose degradation level	Lignin degradation level	Degradation level	Main deterioration driver
NO. 1	Elm	Beam	Indoor; fluctuating relative humidity	15%-30%	30%-50%	Slight	Moderate	Moderate	Fluctuating relative humidity；fungal attack
NO. 2	Willow	Window	Outdoor; weather-exposed	33%-40%	35%-45%	Moderate	Moderate	Moderate	Solar weathering；Insect damage；fungal attack
NO. 3	Poplar	Column	Outdoor; weather-exposed	45%-50%	50%-70%	Moderate	Severe	Severe	Solar weathering；Insect damage；fungal attack
NO. 4	Birch	Purlin	Indoor; fluctuating relative humidity	33%-40%	35%-45%	Moderate	Moderate	Moderate	Fluctuating relative humidity; fungal attack
NO. 5	Birch	Purlin	Indoor; fluctuating relative humidity	33%-40%	35%-45%	Moderate	Moderate	Moderate	Fluctuating relative humidity; fungal attack
NO. 6	Chinese larch	Rafter	Outdoor; weather-exposed	35%-50%	30%-40%	Moderate	Moderate	Moderate	Solar weathering；fungal attack
NO. 7	Chinese larch	Rafter	Outdoor; weather-exposed	35%-50%	30%-40%	Moderate	Moderate	Moderate	Solar weathering；fungal attack
NO. 8	Chinese pine	Purlin	Indoor; fluctuating relative humidity	45%-60%	30%-45%	Moderate	Moderate	Moderate	Fluctuating relative humidity; fungal attack

NO. 9	Chinese larch	Window	Outdoor; weather-exposed	40%-50%	35%-50%	Moderate	Moderate	Moderate	Solar weathering; fungal attack
NO. 10	Willow	Window	Outdoor; weather-exposed	30%-40%	35%-45%	Moderate	Moderate	Moderate	Solar weathering; Insect damage; fungal attack
NO. 11	Poplar	Door	Outdoor; weather-exposed	45%-50%	50%-70%	Moderate	Severe	Severe	Solar weathering; Insect damage; fungal attack
NO. 12	Chinese pine	Door	Outdoor; weather-exposed	45%-60%	30%-45%	Moderate	Moderate	Moderate	Solar weathering; fungal attack
NO. 13	Birch	Beam	Indoor; fluctuating relative humidity	30%-40%	35%-45%	Moderate	Moderate	Moderate	Fluctuating relative humidity; fungal attack
NO. 14	Willow	Beam	Outdoor; weather-exposed	50%-75%	70%-80%	Severe	Severe	Severe	Solar weathering; Insect damage; fungal attack
NO. 15	Willow	Beam	Outdoor; weather-exposed	95%-99%	85%-95%	Severe	Severe	Severe	Solar weathering; Insect damage; fungal attack
NO. 16	Willow	Door	Outdoor; weather-exposed	95%-98%	85%-95%	Severe	Severe	Severe	Solar weathering; Insect damage; fungal attack
NO. 17	Poplar	Rafter	Outdoor; weather-exposed	60%-80%	70%-90%	Severe	Severe	Severe	Solar weathering; Insect damage; fungal attack
NO. 18	Chinese pine	Door	Outdoor; weather-exposed	5%-15%	50%-60%	Slight	Moderate	Moderate	Solar weathering; fungal attack